PHILOSOPHICAL TRANSACTIONS OF THE ROYAL SOCIETY B

rstb.royalsocietypublishing.org

Research

Cite this article: Gómez JM, Perfectti F, Klingenberg CP. 2014 The role of pollinator diversity in the evolution of corolla-shape integration in a pollination-generalist plant clade. *Phil. Trans. R. Soc. B* **369**: 20130257. http://dx.doi.org/10.1098/rstb.2013.0257

One contribution of 14 to a Theme Issue 'Phenotypic integration and modularity in plants and animals'.

Subject Areas:
evolution, ecology, genetics, developmental biology, plant science

Keywords:
geometric morphometrics, floral integration, pollination generalization, *Erysimum*, phylogenetic comparative method

Author for correspondence:
José María Gómez
e-mail: jmgreyes@eeza.csic.es

Electronic supplementary material is available at http://dx.doi.org/10.1098/rstb.2013.0257 or via http://rstb.royalsocietypublishing.org.

Royal Society Publishing

The role of pollinator diversity in the evolution of corolla-shape integration in a pollination-generalist plant clade

José María Gómez[1,2], Francisco Perfectti[3] and Christian Peter Klingenberg[4]

[1]Department of Functional and Evolutionary Ecology, Estación Experimental de Zonas Áridas (EEZA-CSIC), [2]Department of Ecology, and [3]Department of Genetics, University of Granada, Granada, Spain
[4]Faculty of Life Sciences, University of Manchester, Dover Street, Manchester M13 9PL, UK

Flowers of animal-pollinated plants are integrated structures shaped by the action of pollinator-mediated selection. It is widely assumed that pollination specialization increases the magnitude of floral integration. However, empirical evidence is still inconclusive. In this study, we explored the role of pollinator diversity in shaping the evolution of corolla-shape integration in *Erysimum*, a plant genus with generalized pollination systems. We quantified floral integration in *Erysimum* using geometric morphometrics and explored its evolution using phylogenetic comparative methods. Corolla-shape integration was low but significantly different from zero in all study species. Spatial autocorrelation and phylogenetic signal in corolla-shape integration were not detected. In addition, integration in *Erysimum* seems to have evolved in a way that is consistent with Brownian motion, but with frequent convergent evolution. Corolla-shape integration was negatively associated with the number of pollinators visiting the flowers of each *Erysimum* species. That is, it was lower in those species having a more generalized pollination system. This negative association may occur because the co-occurrence of many pollinators imposes conflicting selection and cancels out any consistent selection on specific floral traits, preventing the evolution of highly integrated flowers.

1. Introduction

Flowers of animal-pollinated plants are complex structures that increase fitness by promoting behavioural and morphological matching with pollinators [1,2]. As in most complex structures, the efficacy of a flower in performing its function depends on how accurately all its parts work together. According to this idea, the role of natural selection in favouring the functional coordination of the flower parts has long been acknowledged [3]. In particular, in animal-pollinated plants, it is widely assumed that pollinators play a large role in the evolution of not only floral traits but also floral integration [4–13]. Pollinators, besides affecting the mean and variation of floral traits by exerting directional and stabilizing selection, can also impose correlational selection on certain combinations of floral traits [14,15]. The morphological integration of flowers pollinated by animals is expected to be higher than the integration of wind- and self-pollinated flowers [5–7,10].

Ever since the first quantitative analysis on floral integration was performed, it was predicted that its magnitude would be larger in plant species with specialized pollination systems [13]. It is widely assumed that, while specialized pollination systems strengthen floral integration, generalized pollination systems weaken it, mostly because generalized plants undergo frequent conflicting selection as a consequence of interacting simultaneously with different pollinator functional groups having contrasting morphology, preference and foraging behaviour. Under these circumstances, the local co-occurrence of several pollinator types imposing opposing selection cancels the occurrence of consistent selection on specific floral traits, preventing the evolution of highly integrated flowers [12]. Empirical evidence supporting this early prediction is still scarce and somewhat contradictory. Whereas

some studies are consistent with it in detecting stronger floral integration in specialist than in generalist plant species [12,16], other studies have found unexpectedly tight floral integration in plants with generalized pollination systems [13,17]. These contradictory outcomes may partially be a consequence of having compared integration between unrelated plant species and including covariation between traits not belonging to the same functional module [5,18]. Functional modules are composed of genetically integrated parts that perform a joint function and work independently from other modules [5,19,20]. Species from different lineages may differ not only in functional integration (the integration of functional modules), but also in developmental integration (the covariation between morphological elements due to developmental pattern) [18,19]. Because phylogenetically related species have similar developmental pathways, exploring the correlated evolution of floral integration and pollination generalization in a phylogenetic context would help to unravel whether integration represents an adaptive response to pollinators, or in contrast, it has originated by non-adaptive processes [12,13,21,22]. The main question to be solved from this perspective is if any macroevolutionary change in the diversity of pollinators entails a concomitant change in the magnitude of floral integration.

In this study, we explore the macroevolution of corolla-shape integration across a clade of pollination-generalist species belonging to the genus *Erysimum* L. (Brassicaceae). We use geometric morphometric tools to test whether corolla-shape integration evolved as a consequence of changes in pollinator diversity. We have studied corolla-shape integration rather than the integration of other widely explored traits in Brassicaceae, such as style length, anther exertion, etc., because there is a large amount of empirical evidence showing that pollinators exert strong selection on *Erysimum* corolla shape [23–28]. *Erysimum* species are very generalist in their interaction with pollinators [23–25]. Despite this extreme pollination generalization, the reproductive output of several species is limited by pollinator availability [25,26]. In addition, pollinators are main agents of selection on *Erysimum* corolla shape [27]. They exert not only directional or disruptive/stabilizing selection, but also correlational selection on shape component covariation [27,28]. These findings indicate that pollinators have the ability of selecting for corolla-shape integration in *Erysimum*. However, different pollinators exert contrasting selection on corolla shape through differential preference pattern and morphological fit [28]. For example, whereas some bees prefer to visit corollas with narrow and parallel petals, bee-flies prefer corollas with rounded overlapped petals. Under these circumstances, *Erysimum* species interacting with few pollinators would probably show stronger corolla-shape integration than *Erysimum* species simultaneously visited by many pollinator types. We hypothesize thereby that, despite being pollination generalists, the magnitude of corolla-shape integration in *Erysimum* will be negatively related with the diversity of flower visitors due to an increase in the intensity of conflicting selection. The specific goals of this study are: (i) to estimate the magnitude of corolla-shape integration in *Erysimum* species; (ii) to explore the evolutionary mode of the corolla-shape integration; and (iii) to test the correlated evolution between the magnitude of the corolla-shape integration and the diversity of pollinators visiting the flowers in *Erysimum*.

2. Material and methods

(a) Study species

We have studied 40 *Erysimum* species from Western and Central Europe and Northwest Africa (electronic supplementary material, table S1). They represent more than 85% of the species inhabiting this region [29]. These *Erysimum* species inhabit a diverse array of environments, from pure alpine habitats above the treeline in the Alps, Sierra Nevada, Pyrenees or Atlas mountains, to oak and pine forests in Mediterranean mountains, and lowland and coastal habitats in Central Europe and North Africa.

(b) Phylogenetic relationships among *Erysimum* species

We collected fresh leaf material from one individual of each of 39 *Erysimum* species (electronic supplementary material, table S1; *E. cheiri* was not included in the phylogenetic analysis) directly in the field. In addition, we included *E. passgalense* from Iran in the phylogenetic reconstruction. Leaf tissues were dried and conserved in silica gel until DNA extractions were performed, using the GenElute Plant Genomic DNA miniprep Kit (Sigma-Aldrich) and liquid nitrogen.

One nuclear and two chloroplast DNA regions were amplified and sequenced. The nuclear sequence was composed by the internal transcribed spacers (ITSs) of the ribosomal DNA (*ITS1* and *ITS2*) and the 5.8 rDNA between both ITSs sequences, which jointly span approximately 700 nucleotides. The chloroplast regions involved 2003 nucleotides of the NADH dehydrogenase subunit F (*ndhF)* gene and approximately 1200 nucleotides of the *trnT-trnL* intergenic spacer. Details of the polymerase chain reactions, primers and sequencing have been previously described [30]. Sequences were uploaded to GenBank (accession numbers in the electronic supplementary material, table S2).

Contigs were assembled, revised, aligned and concatenated using Geneious 5 (created by Biomatters; available from http://www.geneious.com/), with posterior manual inspection. A region of indels and poly-A in the central part of the trnT-trnL were identified and excluded using Gblocks server [31] with the less stringent conditions.

We built the phylogenetic tree using Bayesian inference as implemented in MrBayes v. 3.2 [32]. We used *E. passgalense* as outgroup. In addition, we confirmed the suitability of *E. passgalense* as outgroup using *Arabidopsis thaliana* and *Moricandia moricandioides* as more distant outgroups (data not shown). Different evolutionary models were fitted for each DNA region (*ITS1*, *ITS2*, *rDNA*, *ndhF* and *trnT-trnL*) using MrModeltest v. 2.3 [33]. The best fitted models were the JC for *ITS1*, the K80 + G for *ITS2*, the K80 for *5.8S*, the GTR + G for *nadhF* and the F81 + G for the *trnT-trnL* sequence. The Markov chain Monte Carlo (MCMC) chains were run for 2×10^6 generations in two independent runs. Every 500 generations a tree was saved, resulting in 4000 trees for each run. We checked convergence using Tracer v. 1.5 [34] and discarded, as the burn-in phase, the first 20% of the saved trees. The consensus tree was obtained from the final set of 6400 trees.

(c) Pollinator survey

We conducted pollinator counts in one to three georeferenced populations per species in each of 35 species (electronic supplementary material, table S1; we did not obtain data from *E. incanum*, *E. linifolium*, *E. seipkae*, *E. sylvestre* and *E. virgatum*). We visited each population during bloom peak and recorded the insects visiting the flowers, only counting those insects that contacted anthers or stigma at least during part of their visit to the flowers (i.e. they can act as pollinators). Previous studies in some Iberian *Erysimum* indicate that a sample of 130–150 insects provided an accurate estimate of the diversity of the pollinator

assemblage [28]. To standardize sampling effort, we tried to visit each population for the same amount of time, always trying to reach that minimum number of recorded insects. Overall, we sampled each population for 2.5–3 h. Unfortunately, it was impossible to reach this amount of floral visitors in a few populations where insects were especially scarce. However, we kept these populations in our study because we observed that their removal did not change our main outcomes. Pollinators were identified in the field, and some specimens were captured for further identification in the laboratory.

We grouped the insects visiting *Erysimum* flowers in functional groups [35]. We define a 'functional group' as those insects that interact with the flowers in a similar manner. Basically, we used criteria of similarity in body length, proboscis length, foraging behaviour and feeding habits [36]. Thus, taxonomically related species were sometimes placed in different functional groups. We established 20 functional groups: (1) long-tongued large bees: mostly nectar-collecting bees greater than or equal to 10 mm in body length belonging to the families Anthophoridae (mostly *Anthophora* spp.) and Apidae (*Apis mellifera* and several *Bombus* spp.); (2) short-tongued large bees: mostly pollen- and nectar-collecting females greater than 10 mm belonging primarily to the families Halictidae (*Lasioglossum* spp., *Halictus* spp.), Megachilidae (*Osmia* spp.), Colletidae (*Colletes* spp.) and Andrenidae (*Andrena* spp.); (3) short-tongued medium-sized bees: mostly pollen- and nectar-collecting females between 5 and 10 mm also belonging to the families Halictidae (*Lasioglossum* spp., *Halictus* spp.) and Andrenidae (*Andrena* spp.); (4) short-tongued small bees: mostly pollen- and nectar-collecting females less than 5 mm—although they were pollinators, they could act as nectar thieves and belonged primarily to the families Halictidae (*Lasioglossum* spp.), Colletidae (*Hyleaus* spp.), Andrenidae (*Andrena* spp.), Apidae Xylocopinae (*Ceratina* spp.) and Apidae Nomidinae (*Nomada* spp.); (5) short-tongued extra-small bees: mostly pollen- and nectar-collecting females less than 2 mm—although they were pollinators, they could act as nectar thieves and belonged primarily to the families Halictidae (*Lasioglossum* spp.) and Colletidae (*Hyleaus* spp.); (6) ants: both orthodox pollinators and nectar thieves belonging mostly to the genera *Formica*, *Camponotus*, *Proformica*, *Plagiolepis* and *Leptothorax*; (7) large wasps: large aculeate wasps, parasitic wasps, and kleptoparasitic bees collecting only nectar (mostly *Polistes* spp.); (8) small wasps: small parasitic wasps belonging to Chalcidoidea and Ichneumonoidea, collecting only nectar, and acting both as pollinators and nectar thieves; (9) bee-flies: long-tongued nectar-collecting flies while hovering and belonging to the families Bombyliidae (mostly *Bombylius* spp.) and Nemestrinidae; (10) hoverflies: nectar- and pollen-collecting Syrphidae and short-tongued Bombyliidae; (11) large flies: nectar-collecting flies greater than 5 mm, mostly belonging to the families Muscidae, Calliphoridae, Tabanidae, Scatophagidae and Anthomyiidae; (12) small flies: nectar-collecting flies less than 5 mm mostly belonging to families Muscidae, Anthomyiidae, Mycetophilidae, Empididae, Bibionidae, Drosophilidae and Stratiomyidae (these flies, although pollinating the flowers, may also act as nectar thieves); (13) large beetles: including species collecting pollen mostly belonging to the families Scarabaeidae and Alleculidae; (14) small beetles: including species collecting nectar and/or pollen while entering completely into the flower, mostly belonging to the families Melyridae (Malachidae and Dasytidae), Cleridae, Oedemeridae, Nitidulidae, Elateridae, Bruchidae, Buprestidae, Phalacridae and Chrysomelidae; (15) butterflies: mostly Rhopalocera belonging to the families Nymphalidae and Pieridae plus some diurnal moths belonging to the family Sphingidae, all nectar collectors; (16) moths: small nectar-collecting Lepidoptera mostly belonging to the families Adelidae and Incurvariidae; (17) bugs: nectar-collecting Hemiptera belonging mostly to the family Lygaeidae and Pentatomidae (outstanding *Eurydema* spp.; these insects also act as sapsuckers); (18) thrips: small Thysanoptera collecting pollen within the flowers; (19) grasshoppers: pollen-collecting Orthoptera inmatures; and (20) others: some species of snakeflies, earwigs, etc., that visit the flowers to collect both pollen and nectar.

We described the diversity of the flower visitor fauna of the studied plants, both at insect species and functional group levels, using two complementary indices: (1) Pollinator richness (S_{obs}), calculated as the overall number of flower visitor species or functional groups recorded in the flowers of each plant species. To control for sampling effort, we used the average number of insect species visiting the flowers of each species per population. (2) Pollinator diversity, calculated as Hurlbert's PIE, the probability that two randomly sampled insects from the community pertain to two different species or functional groups. This is an evenness index that incorporates the frequency of visitation of functional and taxonomic groups of insects and combines the two mechanistic factors affecting diversity: dominance and species abundance. These indices were generated using the 'addpart' function in R package stratigraph [37].

(d) Magnitude of morphological integration in corolla shape

To quantify the morphological integration of a complex, multidimensional trait such as the *Erysimum* corolla shape, we have used geometric morphometric tools based on a landmark-based methodology [38]. For this, we selected one flower at anthesis per individual plant in each of 37 *Erysimum* species (table 1; see the electronic supplementary material, table S1 for information on sample size per *Erysimum* species; no data on *E. incanum*, *E. seipkae* and *E. virgatum*) and took a digital photo of the front view and planar position. We defined 32 co-planar landmarks covering the corolla shape and using midrib, primary and secondary veins and petal extremes and connections (see [39] for a full description of the methodology). From the two-dimensional coordinates of landmarks, we extracted shape information and computed the generalized orthogonal least-squares Procrustes averages using the Generalized Procrustes Analysis (GPA) superposition method. This analysis was performed in MorphoJ [40].

The morphological integration of the corolla shapes was computed for each *Erysimum* species by calculating the relative variance of eigenvalues (EV) of the respective covariance matrix of Procustes coordinates [41]. One aspect of integration is that variation is concentrated in one or a few of the available dimensions [42]. As a consequence, there will be one or a few large and many small EV for the covariance matrix of integrated data, but EV of the covariance matrix will be more homogeneous for data lacking integration. Following this logic, the variance of EV has been used extensively to quantify integration in correlation matrices of distance measurements [43] and is one of the best measures of morphological integration [44]. In the context of geometric morphometrics, however, covariance matrices must be used, and EV were standardized by the total shape variance to control for among-species differences in the amount of total shape variation [41]. The total variance of shape can be obtained by summing the variances of all Procrustes coordinates for each species. We tested the statistical significance of shape integration by bootstrapping.

(e) Evolution of corolla-shape integration

We explored the evolutionary models better describing the evolution of corolla-shape integration in *Erysimum*. In particular, we tested whether the evolution of corolla-shape integration was associated with a directional trend or with an optimal value. For this, we compared the likelihood of a model assuming a Brownian

Table 1. Summary of the magnitude in corolla-shape and pollinator diversity of the study species. PC, principal component.

species	% variance explained by first PC	shape variance	shape integration	no. floral visitors	pollinator species		pollinator functional groups	
					S_{obs}/ pop.	Hurlbert PIE	S_{obs}	Hurlbert PIE
E. baeticum baeticum	43.00	0.026	0.118	78	26	0.969	18	0.784
E. baeticum bastetanum	32.49	0.032	0.086	56	22	0.488	19	0.488
E. bicolor	36.65	0.025	0.171	19	19	0.540	8	0.486
E. bonannianum	32.66	0.025	0.121	43	22	0.919	15	0.864
E. cazorlense	42.13	0.032	0.226	17	17	0.848	13	0.821
E. cheiranthoides	40.94	0.021	0.169	20	20	0.767	11	0.697
E. cheiri	43.99	0.036	0.156	42	21	0.970	8	0.573
E. collisparsum	43.99	0.026	0.216	14	14	0.854	8	0.710
E. crassistylum	30.88	0.025	0.072	19	11	0.791	7	0.691
E. crepidifolium	42.95	0.039	0.261	25	13	0.897	14	0.870
E. duriaei	33.09	0.025	0.150	30	15	0.937	10	0.646
E. etnense	30.18	0.030	0.144	33	17	0.905	14	0.884
E. fitzii	39.85	0.028	0.092	39	20	0.866	14	0.762
E. geisleri	44.97	0.028	0.208	42	21	0.943	18	0.898
E. gomezcampoi	45.94	0.033	0.134	18	16	0.760	8	0.659
E. gorbeanum	58.08	0.027	0.315	14	14	0.756	10	0.677
E. jugicola	44.14	0.031	0.225	31	16	0.929	13	0.865
E. lagascae	42.72	0.035	0.145	29	15	0.620	13	0.442
E. linifolium	40.68	0.037	0.297					
E. mediohispanicum	35.07	0.044	0.124	120	17	0.965	19	0.841
E. metlesicsii	43.68	0.021	0.178	16	16	0.722	6	0.538
E. merxmuelleri	31.18	0.030	0.072	72	36	0.943	19	0.882
E. myriophyllum	48.09	0.033	0.140	36	18	0.507	14	0.357
E. nervosum	31.85	0.027	0.072	43	22	0.887	15	0.701
E. nevadense	34.41	0.025	0.073	127	25	0.963	20	0.821
E. odoratum	39.04	0.026	0.086	49	25	0.938	18	0.845
E. penyalarense	32.37	0.033	0.198	34	17	0.884	10	0.704
E. popovii	42.13	0.041	0.148	30	15	0.813	10	0.745
E. pseudorhaeticum	35.33	0.027	0.079	35	18	0.904	15	0.783
E. rhaeticum	57.23	0.027	0.167	41	21	0.880	14	0.777
E. riphaeanum	50.06	0.034	0.163	34	17	0.929	17	0.865
E. rondae	31.46	0.035	0.089	26	26	0.858	13	0.742
E. ruscinonense	51.42	0.041	0.204	51	26	0.776	17	0.547
E. scoparium	36.65	0.025	0.171	60	14	0.933	13	0.825
E. semperflorens	43.00	0.042	0.152	20	20	0.909	11	0.809
E. sylvestre	43.32	0.041	0.159					
E. wilczekianum	30.42	0.019	0.045	27	14	0.900	13	0.850

motion (BM) evolution mode (BM model) of the corolla-shape integration with models assuming an evolutionary trend in its rate (trend model) and magnitude of evolution (drift model), and with another model assuming an optimal peak in the evolution of corolla-shape integration (Orstein–Uhlenbeck model, OU) [45]. The BM model assumes that the changes in the value of a trait are independent of previous changes, larger changes are more probable in larger branches and the rate of evolution is constant over time [45]. The trend model is a diffusion model assuming linear trend in rates, towards larger or smaller rates, through time [46]. The drift model is a model assuming a directional component, a trend towards smaller or larger values [46]. The OU model assumes that the trait has an optimum value [45,47]. Different mechanisms are assumed to cause each of these

evolutionary models. Whereas the BM mode of evolution may be the result of either neutral evolution or randomly fluctuating selection, the OU mode may result from stabilizing selection and the trend and above all the drift mode may be a consequence of directional selection [45,48]. These analyses were performed using the 'fitContinuous' command in the R package geiger 1.99–1 [46]. To incorporate phylogenetic uncertainty, we repeated all these analyses for each of the 6400 phylogenetic trees obtained by Bayesian inference, after exclusion of the trees generated in the burn-in phase.

We tested the association between *Erysimum* phylogeny and both the pollinator diversity and corolla-shape integration by estimating their phylogenetic signals using both Blomberg's K and Pagel's λ [49–51]). Blomberg's K expresses the strength of phylogenetic signal as the ratio of the mean squared error of the tip data (MSE_0) measured from the phylogenetic corrected mean and the mean squared error based on the variance–covariance matrix derived from the given phylogeny under the assumption of BM (MSE) [50,51]. In a case in which the similarity of trait values is well predicted by the phylogeny, MSE will be small and thus MSE_0/MSE large. Pagel's λ is a tree transformation that assesses the degree of phylogenetic signal within the trait by multiplying the internal branches of the tree by values ranging between 0 and 1. A λ of 1 indicates a BM model, and the tree is returned with its branch lengths untransformed. A λ of 0 indicates no patterning as the tree is collapsed to a single large polytomy, a star phylogeny [45]. These analyses were performed using the 'phylosig' function in the R package phytool 0.2–14 [52].

To illustrate the phylogenetic signal and evolution mode of corolla-shape integration, we built up a traitgram [53]. Traitgrams arrange species along a continuous trait axis (the x-axis) and connect them with their underlying phylogenetic tree (time on the y-axis) [51]. Internal node positions correspond to ancestral states obtained by maximum likelihood. Node depths reflect phylogenetic branch lengths [53]. Traitgram was performed in the R package paleotree 1.8.1 [54].

We also estimated the ancestral states of the corolla-shape integration incorporating the phylogenetic uncertainty. For that, we performed the analyses with the set of 6400 phylogenetic trees. Ancestral states were estimated both by maximum likelihood and by Bayesian methods. Maximum-likelihood ancestral state reconstruction was done with the 'getAncStates' function in the R package geiger 1.3–1 [46]. This function estimates ancestral character states for continuous characters under a BM model. Bayesian ancestral state reconstruction was done using the 'anc.Bayes' function implemented in the R package phytool 0.2–14 [52]. This function uses Bayesian MCMC to sample from the posterior probability for the states at internal nodes in the tree. The posterior probabilities for each character state at each internal node were obtained with the 'ace' command in R packages ape 3.0–6 [55] and phytool 0.2–14 [52].

(f) Correlated evolution between corolla-shape integration and pollinator diversity

We explored the correlated evolution of corolla-shape integration and pollinator richness (S_{obs}) and diversity (Hurlbert's PIE) using phylogenetic generalized least-square (PGLS) models [45]. Because the sampling effort varied across *Erysimum* species (electronic supplementary material, table S1), we used the number of pollinator species visiting each *Erysimum* species per population as the pollinator richness estimate. In addition, we also explored the correlated evolution of corolla-shape integration and the abundance of each pollinator functional group per plant species by performing a PGLS model including as independent variables the abundance of each functional group representing more than 5% of the total visits. To control for among-*Erysimum* differences in sampling effort, we included as covariate in the PGLS the number of individual plants analysed per species. Furthermore, we included as explanatory variables the longitude and latitude of each population, to control for spatial dependence [52,56]. We used this approach, rather than spatially controlled residuals, following a suggestion made by Freckleton [57]. We allow both λ and δ transformation to be optimized by maximum likelihood while fitting the model. Lambda (λ) scales the internal branches moving from 1 and 0 in a way that when λ is 1 the tree is returned unchanged (BM model), and when λ is 0 the internal branches become smallest and all the branches emanate from a common node in a star phylogeny [49]. Delta (δ) transforms the node heights of the phylogeny in a way that when $\delta > 1$ it increases the length of external nodes and thus models a scenario where rates of evolution increase through time, whereas $\delta < 1$ decreases the length of external nodes and thus models a scenario where rates of evolution decrease through time [49]; $\delta = 1$ is a BM model and the tree is returned unchanged. Furthermore, we considered the phylogenetic uncertainty by repeating the PGLS for each of the 6400 phylogenetic trees. All the analyses were performed using the R package caper 0.2 [58].

3. Results

(a) Phylogenetic relationships among *Erysimum* species

The phylogenetic analysis suggests that *E. incanum* and the North-African alpine species *E. wilczekianum* are basal to the rest of the studied species of *Erysimum* (electronic supplementary material, figure S1). There are two well-supported clades among the remaining species of *Erysimum*. A first monophyletic clade includes *Erysimum* species from the Alps (*E. sylvestre*), Italian Peninsula, Sicily and Moroccan Rif Mountains (*E. riphaeanum*) (electronic supplementary material, figure S1). The other clade includes the species from the Iberian Peninsula and the Macaronesia and the two remaining North-African wallflowers (electronic supplementary material, figure S1). This latter clade is subdivided into several well-supported subclades (electronic supplementary material, figure S1).

(b) Pollinator diversity

We recorded a total 13 724 flower visits to the studied populations, comprising 1393 pairwise insect–plant interactions from 746 insect species belonging to 99 families and eight orders (electronic supplementary material, appendix S1). The top 10 most abundant flower visitors were the long-tongue large bees *Anthophora aestivalis* (Anthophoridae; 524 records), *A. alluaudi* (373 records) and *A. leucophaea* (335 records); the bee-flies *Bombylius major* (Bombyliidae; 517 records) and *B. fulvescens* (399 records); the beetles *Meligethes maurus* (Nitidulidae; 474 records), *M. aeneus* (473 records) and *Dasytes subaeneus* (Melyridae; 230 records); the ant *Plagiolepis schmitzii* (Formicidae; 569 records) and the butterfly *Vanessa cardui* (Nymphalidae; 202 records).

All *Erysimum* species were very generalist. The average number of insect species visiting their flowers per plant population was 19 ± 5, ranging between 11 in *E. crassistylum* and 36 in *E. merxmuelleri* (table 1), whereas the average number of functional groups visiting the *Erysimum* flowers was 13 ± 4, ranging between six in *E. metlesicsii* and 20 in *E. nevadense* (table 1). That is, no *Erysimum* species was visited by just one or two functional groups of insects, and they cannot thereby be classified as bee-fly-pollinated species,

butterfly-pollinated species, etc. (electronic supplementary material, appendix S1).

Furthermore, pollinator assemblage was still very diverse when taking into account not only the number of species or functional groups at flowers but also their relative abundances. The average Hurlbert's PIE of insect species was 0.84 ± 0.13, ranging between 0.54 in *E. bicolor* and 0.97 in *E. baeticum baeticum* and *E. cheiri* (table 1). Similarly, the average Hurlbert's PIE of insect functional groups was 0.74 ± 0.14, ranging between 0.36 in *E. myriophyllum* and 0.90 in *E. geisleri*. That is, a decrease in taxonomic, specific diversity of pollinators was not due to a decrease in the functional groups of the floral visitors. There was not functional specialization in the pool of species used in this study.

We did not find spatial autocorrelation either in the richness ($r = -0.13$, $p = 0.980$, Mantel test) or diversity ($r = 0.07$, $p = 0.990$, Mantel test) of insect species. There was not either phylogenetic signal in the richness (Blomberg's $K = 0.106$, $p = 0.901$; Pagel's $\lambda = 0.0001$, $p = 0.999$) or diversity (Blomberg's $K = 0.139$, Pagel's $p = 0.866$; $\lambda = 0.0001$, $p = 0.999$) of insect species (similar outcomes with insect functional groups, data not shown).

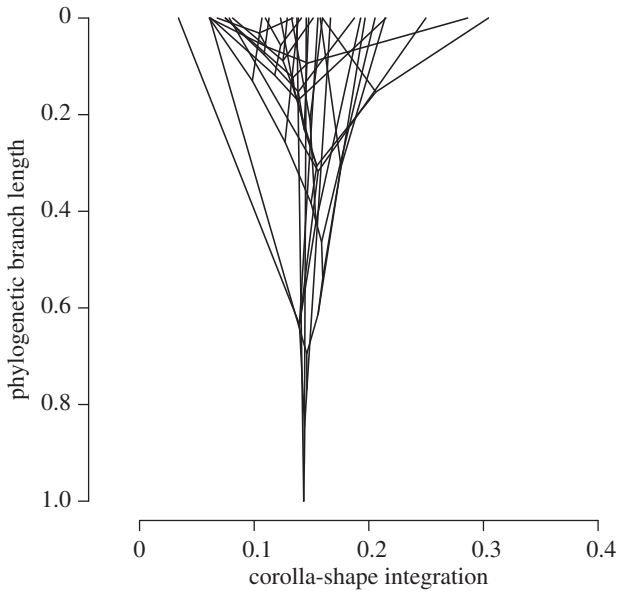

Figure 1. Traitgram showing the changes in the magnitude of corolla-shape integration in relation to the phylogenetic relatedness of the *Erysimum* species.

(c) Morphological integration of corolla shape

The average proportion of shape variance explained by the first principal component (PC), pooling all species, was $40.3 \pm 7.2\%$ ($N = 37$ spp.). However, there was across-species variation in this value, ranging between 30.2% in *E. etnense* and 58.1% in *E. gorbeanum* (table 1), with an across-species coefficient of variation of 18.1%. Corolla-shape variance was 0.031 ± 0.006, ranging between 0.019 in *E. wilczekianum* and 0.044 in *E. mediohispanicum* (across-species coefficient of variation, CV = 20.6%) (electronic supplementary material, figure S2).

The average magnitude of corolla-shape integration, when pooling all *Erysimum* species, was 0.15 ± 0.06 (table 1). The integration value was significant for all *Erysimum* species except *E. wilczekianum* at $\alpha < 0.05$ according to a bootstrapping resampling. As found in previous variables, corolla integration also varied between species, ranging between 0.04 in *E. wilczekianum* and 0.31 in *E. gorbeanum* (across-species CV = 42.0%; table 1).

(d) Evolution mode of corolla-shape integration

There is no evidence of a directional trend in the rate or magnitude of the evolution of corolla-shape integration, as there was no phylogenetic tree ($N = 6400$ trees) where the data fitted better to a trend ($\ln L = 39.8 \pm 2.3$; AIC $= -73.7 \pm 4.6$) or drift model ($\ln L = 49.9 \pm 0.1$; AIC $= -91.6 \pm 0.3$) than to a BM model ($\ln L = 49.8 \pm 0.1$; AIC $= -93.6 \pm 0.1$). In addition, no evidence exists of an optimal value in the evolution of the corolla-shape integration, since there was no single tree obtaining a significant p-value associated with the difference in log likelihoods between OU ($\ln L = 50.5 \pm 0.2$; AIC $= -95.1 \pm 0.5$) and BM models.

Nevertheless, our results suggest that the evolution of corolla-shape integration does not fit to a pure BM model, because there was no phylogenetic signal in the morphological integration of *Erysimum* corolla shape. The absence of phylogenetic signal was apparent whether tested with Blomberg' K (0.22 ± 0.05, all p-values > 0.05, 6400 trees) or Pagel's λ (0.0006 ± 0.01, all p-values > 0.05, 6400 trees). The extremely small value of λ even suggests that integration is evolving in each *Erysimum* species in a phylogenetically independent way. Accordingly, the traitgram shows many crossings in corolla-shape integration values (figure 1).

The corolla-shape integrations of ancestral nodes were estimated by maximum-likelihood and Bayesian inference analyses, and both methods showed similar results. As observed in figure 2, these two methods estimated that the corolla-shape integration of ancestral nodes was 0.14. In addition, the integration of the internal nodes ranged between 0.14 and 0.17 (electronic supplementary material, tables S3 and S4). This is a small variation, taking into account that the corolla-shape integration of the studied *Erysimum* species ranged between 0.04 and 0.31. This finding agrees with previous results and suggests that most changes in corolla-shape integration have probably occurred very fast and close to the tips of the phylogenetic tree.

(e) Correlated evolution between corolla-shape integration and pollinator diversity

There was a consistently negative relationship between the number of insect species visiting the flowers of each *Erysimum* species and the integration of their corolla shape (estimate $= -0.05 \pm 0.006$, $N = 6400$ phylogenetic trees and 34 species, excluding *E. cheiri*, *E. linifolium*, *E. virgatum*, *E. seipkae*, *E. sylvestre* and *E. incanum*; figure 3*a*). In fact, only in three out of the 6400 phylogenetic trees was there a positive relationship between pollinator richness and corolla-shape integration (figure 3*b*). In addition, the relationship between corolla-shape integration and pollinator richness was significant at $p < 0.05$ in 5066 trees (79%) and marginally significant at $p < 0.1$ in 6390 trees (99.8%; figure 3*b*). The average value of λ was 0.001 ± 0.033, significantly differing from 1 (p-value $= 0.001 \pm 0.01$) but not from zero (p-value $= 0.99 \pm 0.03$). The average value of δ was 0.51 ± 0.29, significantly differing from 1 (p-value testing λ departure from $1 = 0.02 \pm 0.09$) as well as from zero (p-value testing λ departure from $0 = 0.0001 \pm 0.0000$).

By contrast, we did not find significant relationship between corolla-shape integration and Hurlbert's PIE estimate of

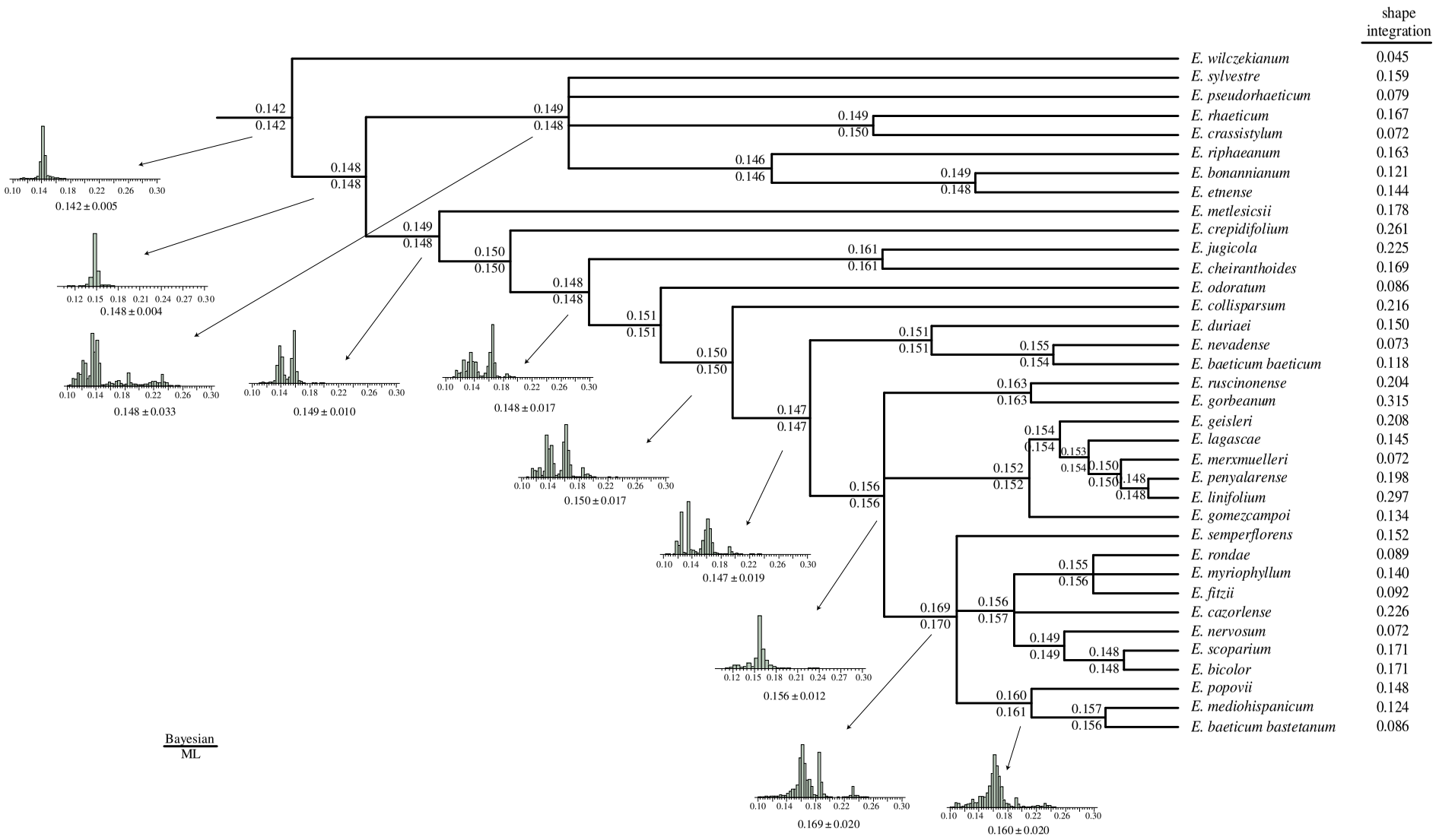

Figure 2. Ancestral reconstruction of corolla-shape integration by means of maximum-likelihood and Bayesian inference. In all cases, ancestral reconstruction has been performed on the 6400 phylogenetic trees. The histograms represent the Bayesian reconstruction of the corolla-shape integration across the 6400 phylogenetic trees in some internal nodes. (Online version in colour.)

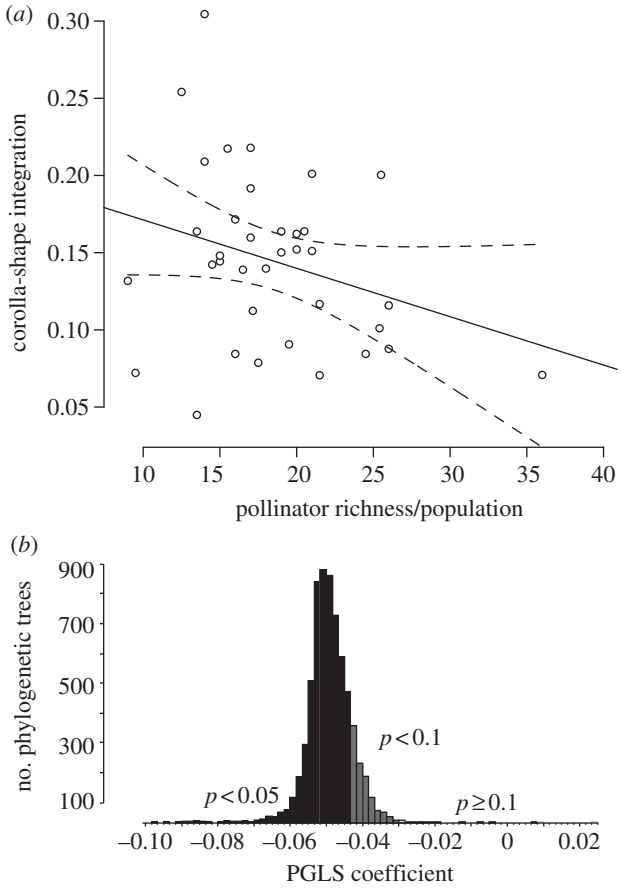

Figure 3. (*a*) Relationship between corolla-shape integration and pollinator richness (expressed as number of flower visitor species per plant population). Line is conventional (non-phylogenetic) least-squares linear regression. (*b*) Distribution of the values of the PGLS coefficients relating corolla-shape integration and pollinator richness in the collection of 6400 phylogenetic trees. The probability values of the subset of PGLS models are: $p < 0.05$, $p < 0.1$ and $p > 0.1$.

pollinator diversity both at species (estimate $= -0.001 \pm 0.001$, all p-values > 1; $\lambda = 0.83 \pm 0.05$, $\delta = 0.92 \pm 0.29$; $N = 34$ species and 6400 phylogenetic trees) or functional group level (estimate $= -0.02 \pm 0.01$, all p-values > 1; $\lambda = 0.0002 \pm 0.01$, $\delta = 0.71 \pm 0.31$; $N = 34$ species and 6400 phylogenetic trees), although in both cases the relationship was negative.

There was no strong relationship between the relative abundance of major flower visitor functional groups (those accounting for more than 5% of the flower visits per plant species) and corolla-shape integration across *Erysimum* species (table 2). However, the effect of all these major pollinator functional groups and corolla integration was positive. That is, the magnitude of corolla integration increases when the pollinator assemblage is dominated by a particular functional group, irrespective of its identity or pollination efficiency.

4. Discussion

(a) The magnitude of floral integration in a supergeneralist plant clade

Our results suggest that corollas in *Erysimum* are integrated traits. *Erysimum* pollinators exert intense selection on their floral traits. In particular, pollinators generate complex patterns of selection on *Erysimum* corolla shape [27]. Pollinators do not only select for individual shape components (relative warps or PCs), but also exert correlational selection that affects both the covariation between these components as well as the whole corolla shape as a single multidimensional trait [27]. These findings suggest that pollinators may theoretically shape the evolution of corolla integration in *Erysimum*. The corolla's contribution to fitness depends on its ability to attract efficient pollinators or to improve their per-visit effectiveness. This function depends highly on the coordinated activity of the different parts of the corolla in order to resemble more precisely the corolla shape favoured by the pollinators. That is, the corolla in *Erysimum*, as presumably in all angiosperms, functions as a single, albeit complex, trait.

Nevertheless, the magnitude of corolla-shape integration was very low in *Erysimum* compared with other angiosperms [10,59]. This is remarkable, because the shape of the corolla undoubtedly works as a single trait. Rosas-Guerrero *et al.* [12] have recently shown that floral traits involved in pollinator attraction tend to show lower integration than those traits related to pollen placement and pick-up. In addition, other traits have proved to be highly integrated in Brassicaceae, such as style length, stamen length, etc. [60]. So, there is some possibility that we are underestimating integration in *Erysimum* flowers by exploring it in a naturally low-integrated trait. Several reasons may explain why we found so low an integration magnitude in *Erysimum* corolla shape.

First, whereas all previous studies have calculated floral integration focusing on standard linear traits, we have calculated integration using a geometric morphometric approach. In this respect, the magnitude of integration found for *Erysimum* is similar to that found in other geometric morphometric studies [41,61]. In fact, the proportion of the total variation in corolla shape explained by the first PC (up to 57% in some species) is similar to that found in highly integrated structures, such as plant leaves [62], hominin dentition [61] or bird cranium [63].

Second, all *Erysimum* species considered in this study were extremely generalist in their interactions with pollinators (see also [24,25]). The number and diversity of insects visiting their flowers was very high even within plant populations. Plants from a single population interacted simultaneously with several functional groups of flower visitors. Owing to the differences in morphology, foraging behaviour and preference pattern, this diversity of pollinators surely prompts the occurrence of conflicting selection on corolla shape. For example, whereas large bees favour corollas with narrow and parallel petals, bee-flies prefer corollas with rounded overlapped petals such as in *E. mediohispanicum* [64]. Although pollinators differ in pollination effectiveness [36], even low-efficiency functional groups, such as beetles, are able to exert significant selection on corolla shape [27]. In fact, as observed in table 2, there was a positive relationship between corolla-shape integration and the abundance of every type of pollinator, even low-efficiency pollinators. This suggests that increasing the abundance of a given pollinator type will entail an increase in floral integration, irrespective of the effectiveness of that pollinator type. Under these circumstances, the local co-occurrence of several pollinator functional groups cancels out the occurrence of consistent selection on a single type of corolla, preventing the evolution of highly integrated corollas.

A third reason why corolla shape may display a low level of integration in *Erysimum* may be related to being visited by inaccurate pollinators that provide inconsistent selection

Table 2. Effect of the relative abundance of each flower visitor functional group on the corolla-shape integration in *Erysimum* considering phylogenetic uncertainty (6400 phylogenetic trees). Only those functional groups accounting for more than 5% of the visits per plant species were included in the analysis. The mean ± 1 s.d. [95% CIs] of the PGLS coefficients between each functional group and integration from the 6400 phylogenetic trees are shown. Also shown is the percentage of phylogenetic trees obtaining significant coefficients at $p < 0.05$ and $p < 0.1$.

flower visitor functional group	estimate ± s.d. [95% CI]	*p*-value ± s.d. [95% CI]	$p < 0.05$ (%)	$p < 0.1$ (%)
long-tongued large bees	0.001 ± 0.0003 [0.001–0.0012]	0.221 ± 0.112 [0.216–0.226]	4.8	10.8
short-tongued large and medium bees	0.001 ± 0.0004 [0.00007–0.0001]	0.802 ± 0.152 [0.795–0.809]	0.3	0.4
short-tongued small and extra-small bees	0.002 ± 0.0003 [0.0019–0.0020]	0.115 ± 0.079 [0.111–0.118]	8.7	44.7
ants	0.001 ± 0.0003 [0.0008–0.0009]	0.447 ± 0.132 [0.441–0.543]	1.1	2.2
bee-flies	0.001 ± 0.0005 [0.0010–0.0011]	0.436 ± 0.188 [0.427–0.444]	2.5	5.5
hoverflies	0.001 ± 0.0008 [0.0005–0.0006]	0.706 ± 0.211 [0.700–0.716]	2.2	3.0
large and small beetles	0.001 ± 0.0006 [0.0012–0.0013]	0.238 ± 0.154 [0.232–0.246]	3.4	10.7
butterflies	0.001 ± 0.0005 [0.0013–0.0014]	0.305 ± 0.129 [0.299–0.311]	2.2	6.5

or that are unable to precisely collect pollen from anthers and deliver it to stigma. In this sense, functional groups of pollinators differ in effectiveness at least in some *Erysimum* species. So, in *E. mediohispanicum*, bees are more efficient than flies and beetles [36]. We think, however, that this is not a main reason explaining low integration in *Erysimum* corollas since we found a relationship between proportion of visits and integration level even for low-efficiency pollinators (table 2).

(b) How does corolla-shape integration evolve in *Erysimum*?

No macroevolutionary trend was found in the evolution of *Erysimum* corolla-shape integration, as the models assuming linear trend in the rates and values of *Erysimum* corolla-shape integration performed poorer than the BM model. This finding suggests that the current evolution of corolla-shape integration in *Erysimum* cannot be explained by invoking long-term, across-species directional selection. Similarly, it seems that corolla-shape integration has not evolved towards a single optimal peak in *Erysimum*, since the OU model also performed worse than the BM model. It seems that the selective factors driving the evolution of corolla-shape integration in *Erysimum* have not been temporally consistent. Both the Bayesian and maximum likelihood ancestral reconstructions of corolla-shape integration suggest that the evolution of this trait has happened very recently in *Erysimum*. Most internal nodes, even shallower nodes, were reconstructed as having an integration level ranging between 0.14 and 0.17, whereas corolla-shape integration of current species well exceeded these bounds (0.04–0.32). Evidence of rapid evolution has grown in recent times [65]. For example, the size of the World's largest flower, *Rafflesia arnoldii*, has apparently evolved very recently [66]. Our study suggests that rapid evolution may involve not only trait values but also trait integration.

The BM mode of trait evolution may be produced by several processes, such as neutral evolution caused by random drift, punctuated change with long static periods interrupted by abrupt changes in trait values, or fluctuating directional selection where the optimal value of the trait may change among species as a consequence of changes in selective scenarios [45,48]. However, pure BM evolution is associated with high phylogenetic signal [53]. In addition, different mechanisms produce different values of phylogenetic signal. In particular, neutral evolution fuelled by genetic drift tends to produce strong phylogenetic signal [52]. However, we found very low phylogenetic signal in *Erysimum* corolla-shape integration, 0.22 quantified as Blomberg's K and 0.0006 as Pagel's λ. So, we presume that other factors rather than genetic drift have driven the evolution of this trait. Low phylogenetic signal in floral integration patterns has been associated with the action of natural selection imposed by pollinators [7]. Revell *et al*. [67] found, through simulation studies, that phylogenetic signal is consistently low under punctuated divergent selection, that is, when daughter lineages evolve to two different optima after every bifurcation. This process may happen when the two daughter lineages face different selective scenarios. Under these circumstances, recurrent short-term divergent selection may cause a macroevolutionary pattern of convergent evolution associated with low phylogenetic signal [53]. According to this, the high frequency of branch crossing found in the traitgram (figure 1) suggests the occurrence of frequent convergent evolution in corolla-shape integration [53]. Some factors mediating corolla-shape integration have presumably changed along the *Erysimum* clade in a fluctuating way, causing the observed pattern of convergence in this trait.

Pollinators are main agents driving floral integration. There is a growing body of empirical evidence suggesting that flowers are indeed highly integrated in specialist plant species [5,8,10–12]. In this sense, Rosas-Guerrero *et al*. [12] have recently reported that integration magnitude sharply decreases from specialist to generalist species in *Ipomoea*. We found a similar pattern along the *Erysimum* genus. As mentioned above, *Erysimum* species are pollinated by a very diverse myriad of insects and, consequently, express a very low magnitude of floral integration. However, despite this rampant generalization, the magnitude of corolla-shape integration was negatively associated with the number and diversity of pollinators visiting the flowers of each *Erysimum* species. That is, even although corolla-shape integration was consistently low in *Erysimum*, it was lower in those species

having a more generalized pollination system. We postulate that this pattern occurs because an increase in pollinator diversity leads to an increase in the intensity and frequency of conflicting selection affecting the corolla shape. This happens because different floral visitors select for different corolla shapes in *Erysimum* [64]. Under these circumstances, no single shape is favoured in the population, causing an increase in shape variability and consequently a decrease in shape integration.

We believe that the evolution of corolla integration has tracked the evolutionary changes in generalization level along the *Erysimum* clade. Indeed, the macroevolutionary pattern of pollination richness evolution was very similar to that found in corolla-shape integration. So, the absence of spatial dependence and phylogenetic signal in pollinator diversity as well as the presence of multiple branch crossing in a traitgram describing its evolution (electronic supplementary material, figure S3) suggests the occurrence of rapid evolution and recurrent convergence in the generalization level of *Erysimum*. It seems that the level of pollination generalization is evolutionarily labile in this genus, changing across species very quickly and without strong phylogenetic and/or geographical limitation. Floral integration has probably been affected by these evolutionary dynamics, increasing in those taxa evolving towards more restricted pollinator assemblages and decreasing in those others evolving towards more generalized pollination systems.

Altogether, our study suggests that pollinators play a role in the evolution of floral integration in this generalist plant clade. Further evidence is necessary to conclude whether the pattern found in this study is idiosyncratic of the *Erysimum* genus or can also occur in other plant clades with generalized pollination systems.

Acknowledgements. We deeply thank Jordi Bosch, Juan Lorite, Mohamed Abdelaziz, Juande Fernández, A. Jesús Muñoz Pajares and Belén Herrador for their help in the field and laboratory. We would like to thank several specialists who kindly identified pollinator specimens: M. A. Alonso Zarazaga, M. Baena, J. Bosch, M. Carles-Tolrà, R. Constantin, S. Fernández Gayubo, M. Goula, F. Gusenleitner, J. Háva, P. Leblanc, M. A. Marcos, F. J. Ortiz Sánchez, J. C. Otero, J. Pérez López, A. Sánchez Ruiz, A. Sánchez Terrón, M. Schwarz, A. Tinaut, F. Vallhonrat and D. Ventura. The Ministerio de Medio Ambiente and Consejerías de Medio Ambiente of Andalucía, Castilla y León, Cataluña and Aragón, as well as the Sierra Nevada National Park Headquarter, granted permission to work in several protected areas of Spain. We thank UGRGRID (University of Granada) for computing facilities.

Funding statement. This study was partially supported by grants from the Spanish MCyT (CGL2009–07015 and CGL2012–34736), MONTES Consolider-Ingenio (CSD2008–00040) and Junta de Andalucía (P07-RNM-02869 and P11-RNM-7676) and was partially supported by EU FEDER funds.

References

1. Harder LD, Barret SC. 2006 *Ecology and evolution of flowers*. Oxford, UK: Oxford University Press.
2. Willmer P. 2011 *Pollination and floral ecology*. Princeton, NJ: Princeton University Press.
3. Darwin C. 1862 *On the various contrivances by which British and foreign orchids are fertilised by insects and on the good effect of intercrossing*. London, UK: Murray.
4. Berg RL. 1960 The ecological significance of correlation pleiades. *Evolution* **14**, 171–180. (doi:10.2307/2405824)
5. Armbruster S, Pelabon C, Hansen T, Mulder C. 2004 Floral integration, modularity, and accuracy: distinguishing complex adaptations from genetic constraints. In *Phenotypic integration: studying the ecology and evolution of complex phenotypes* (eds M Pigliucci, K Preston), pp. 23–49. New York, NY: Oxford University Press.
6. Anderson IA, Busch JW. 2006 Relaxed pollinator-mediated selection weakens floral integration in self-compatible taxa of *Leavenworthia* (Brassicaceae). *Am. J. Bot.* **93**, 860–867. (doi:10.3732/ajb.93.6.860)
7. Pérez F, Arroyo MTK, Medel R. 2007 Phylogenetic analysis of floral integration in *Schizanthus* (Solanaceae): does pollination truly integrate corolla traits? *J. Evol. Biol.* **20**, 1730–1738. (doi:10.1111/j.1420-9101.2007.01393.x)
8. Pérez-Barrales R, Arroyo J, Armbruster SW. 2007 Differences in pollinator faunas may generate geographic differences in floral morphology and integration in *Narcissus papyraceus* (Amaryllidaceae). *Oikos* **116**, 1904–1918. (doi:10.1111/j.0030-1299.2007.15994.x)
9. Bissell EK, Diggle PK. 2008 Floral morphology in *Nicotiana*?: architectural and temporal effects on phenotypic integration. *Int. J. Plant Sci.* **169**, 225–240. (doi:10.1086/523875)
10. Ordano M, Fornoni J, Boege K, Domínguez CA. 2008 The adaptive value of phenotypic floral integration. *New Phytol.* **179**, 1183–1192. (doi:10.1111/j.1469-8137.2008.02523.x)
11. Armbruster WS, Hansen TF, Pélabon C, Pérez-Barrales R, Maad J. 2009 The adaptive accuracy of flowers: measurement and microevolutionary patterns. *Ann. Bot.* **103**, 1529–1545. (doi:10.1093/aob/mcp095)
12. Rosas-Guerrero V, Quesada M, Armbruster WS, Pérez-Barrales R, Smith SD. 2011 Influence of pollination specialization and breeding system on floral integration and phenotypic variation in *Ipomoea*. *Evolution* **65**, 350–364. (doi:10.1111/j.1558-5646.2010.01140.x)
13. Armbruster WS, Stilio VSD, Tuxill JD, Flores TC, Runk JLV. 1999 Covariance and decoupling of floral and vegetative traits in nine Neotropical plants: a re-evaluation of Berg's correlation-pleiades concept. *Am. J. Bot.* **86**, 39–55. (doi:10.2307/2656953)
14. Gómez JM. 2000 Phenotypic selection and response to selection in *Lobularia maritima*: importance of direct and correlational components of natural selection. *J. Evol. Biol.* **13**, 689–699. (doi:10.1046/j.1420-9101.2000.00196.x)
15. Maad J. 2000 Phenotypic selection in hawkmoth-pollinated *Platanthera bifolia*: targets and fitness surfaces. *Evolution* **54**, 112–123. (doi:10.1111/j.0014-3820.2000.tb00012.x)
16. Meng J-L, Zhou X-H, Zhao Z-G, Du G-Z. 2008 Covariance of floral and vegetative traits in four species of Ranunculaceae: a comparison between specialized and generalized pollination systems. *J. Integr. Plant Biol.* **50**, 1161–1170. (doi:10.1111/j.1744-7909.2008.00722.x)
17. Edwards CE, Weinig C. 2011 The quantitative-genetic and QTL architecture of trait integration and modularity in *Brassica rapa* across simulated seasonal settings. *Heredity* **106**, 661–677. (doi:10.1038/hdy.2010.103)
18. Pigliucci M. 2003 Phenotypic integration: studying the ecology and evolution of complex phenotypes. *Ecol. Lett.* **6**, 265–272. (doi:10.1046/j.1461-0248.2003.00428.x)
19. Cheverud JM. 1996 Developmental integration and the evolution of pleiotropy. *Am. Zool.* **36**, 44–50. (doi:10.1093/icb/36.1.44)
20. Klingenberg CP. 2008 Morphological integration and developmental modularity. *Annu. Rev. Ecol. Evol. Syst.* **39**, 115–132. (doi:10.1146/annurev.ecolsys.37.091305.110054)
21. Herrera CM. 2001 Deconstructing a floral phenotype: do pollinators select for corolla integration in *Lavandula latifolia*? *J. Evol. Biol.* **14**, 574–584. (doi:10.1046/j.1420-9101.2001.00314.x)
22. Herrera CM, Cerdá X, García MB, Guitián J, Medrano M, Rey PJ, Sánchez-Lafuente AM. 2002 Floral integration, phenotypic covariance structure and pollinator variation in bumblebee-pollinated *Helleborus foetidus*. *J. Evol. Biol.* **15**, 108–121. (doi:10.1046/j.1420-9101.2002.00365.x)
23. Gómez JM, Bosch J, Perfectti F, Fernández J, Abdelaziz M. 2007 Pollinator diversity affects plant

reproduction and recruitment: the tradeoffs of generalization. *Oecologia* **153**, 597–605. (doi:10.1007/s00442-007-0758-3)

24. Lay CR, Linhart YB, Diggle PK. 2011 The good, the bad and the flexible: plant interactions with pollinators and herbivores over space and time are moderated by plant compensatory responses. *Ann. Bot.* **108**, 749–763. (doi:10.1093/aob/mcr152)
25. Fernández JD, Bosch J, Nieto-Ariza B, Gómez JM. 2012 Pollen limitation in a narrow endemic plant: geographical variation and driving factors. *Oecologia* **170**, 421–431. (doi:10.1007/s00442-012-2312-1)
26. Gomez JM, Abdelaziz M, Lorite J, Jesus Munoz-Pajares A, Perfectti F. 2010 Changes in pollinator fauna cause spatial variation in pollen limitation. *J. Ecol.* **98**, 1243–1252. (doi:10.1111/j.1365-2745.2010.01691.x)
27. Gomez JM, Perfectti F, Camacho JPM. 2006 Natural selection on *Erysimum mediohispanicum* flower shape: insights into the evolution of zygomorphy. *Am. Nat.* **168**, 531–545. (doi:10.1086/507048)
28. Gómez JM, Perfectti F, Bosch J, Camacho JPM. 2009 A geographic selection mosaic in a generalized plant–pollinator–herbivore system. *Ecol. Monogr.* **79**, 245–263. (doi:10.1890/08-0511.1)
29. Heywood VH, Valentine DH, Tutin TG, Burges NA. 1964 *Flora Europaea*. Cambridge, UK: Cambridge University Press.
30. Abdelaziz M, Lorite J, Muñoz-Pajares AJ, Herrador MB, Perfectti F, Gómez JM. 2011 Using complementary techniques to distinguish cryptic species: a new *Erysimum* (Brassicaceae) species from North Africa. *Am. J. Bot.* **98**, 1049–1060. (doi:10.3732/ajb.1000438)
31. Castresana J. 2000 Selection of conserved blocks from multiple alignments for their use in phylogenetic analysis. *Mol. Biol. Evol.* **17**, 540–552. (doi:10.1093/oxfordjournals.molbev.a026334)
32. Ronquist F *et al*. 2012 MrBayes 3.2: efficient Bayesian phylogenetic inference and model choice across a large model space. *Syst. Biol.* **61**, 539–542. (doi:10.1093/sysbio/sys029)
33. Nylander JAA. 2004 *MrModeltest v2*. Uppsala, Sweden: Evolutionary Biology Centre, Uppsala University. See https://github.com/nylander/MrModeltest2.
34. Rambaut A, Drummond AJ. 2007 *Tracer*. See http://tree.bio.ed.ac.uk/software/tracer/.
35. Fenster CB, Armbruster WS, Wilson P, Dudash MR, Thomson JD. 2004 Pollination syndromes and floral specialization. *Annu. Rev. Ecol. Syst.* **35**, 375–403. (doi:10.1146/annurev.ecolsys.34.011802.132347)
36. Gómez JM, Muñoz-Pajares AJ, Abdelaziz M, Lorite J, Perfectti F. 2014 Evolution of pollination niches and floral divergence in the generalist plant *Erysimum mediohispanicum*. *Ann. Bot*. **113**, 237–249. (doi:10.1093/aob/mct186)
37. Green WA. 2012 *stratigraph: Toolkit for the plotting and analysis of stratigraphic and palaeontological data*. See http://cran.r-project.org/web/packages/stratigraph/index.html.
38. Zelditch ML, Swiderski DL, Sheets HD. 2012 *Geometric morphometrics for biologists: a primer*. Amsterdam, The Netherlands: Elsevier.
39. Gómez JM, Perfectti F. 2010 Evolution of complex traits: the case of *Erysimum* corolla shape. *Int. J. Plant Sci.* **171**, 987–998. (doi:10.1086/656475)
40. Klingenberg CP. 2011 MorphoJ: an integrated software package for geometric morphometrics. *Mol. Ecol. Resour.* **11**, 353–357. (doi:10.1111/j.1755-0998.2010.02924.x)
41. Young NM. 2006 Function, ontogeny and canalization of shape variance in the primate scapula. *J. Anat.* **209**, 623–636. (doi:10.1111/j.1469-7580.2006.00639.x)
42. Klingernberg CP. 2013 Cranial integration and modularity: insights into evolution and development from morphometric data. *Hystrix* **24**, 16. (doi:10.4404/hystrix-24.1-6367)
43. Wagner GP. 1984 On the eigenvalue distribution of genetic and phenotypic dispersion matrices: evidence for a nonrandom organization of quantitative character variation. *J. Math. Biol.* **21**, 77–95. (doi:10.1007/BF00275224)
44. Haber A. 2011 A comparative analysis of integration indices. *Evol. Biol.* **38**, 476–488. (doi:10.1007/s11692-011-9137-4)
45. Nunn CL. 2011 *The comparative approach in evolutionary anthropology and biology*. Chicago, IL: University of Chicago Press.
46. Harmon L *et al*. 2013 *geiger: Analysis of evolutionary diversification*. See http://cran.r-project.org/web/packages/geiger/index.html.
47. Hansen TF. 1997 Stabilizing selection and the comparative analysis of adaptation. *Evolution* **51**, 1341. (doi:10.2307/2411186)
48. O'Meara BC, Ané C, Sanderson MJ, Wainwright PC. 2006 Testing for different rates of continuous trait evolution using likelihood. *Evolution* **60**, 922–933. (doi:10.1111/j.0014-3820.2006.tb01171.x)
49. Pagel M. 1999 Inferring the historical patterns of biological evolution. *Nature* **401**, 877–884. (doi:10.1038/44766)
50. Blomberg SP, Garland T, Ives AR. 2003 Testing for phylogenetic signal in comparative data: behavioral traits are more labile. *Evolution* **57**, 717–745. (doi:10.1111/j.0014-3820.2003.tb00285.x)
51. Münkemüller T, Lavergne S, Bzeznik B, Dray S, Jombart T, Schiffers K, Thuiller W. 2012 How to measure and test phylogenetic signal. *Methods Ecol. Evol.* **3**, 743–756. (doi:10.1111/j.2041-210X.2012.00196.x)
52. Revell LJ. 2012 phytools: an R package for phylogenetic comparative biology (and other things). *Methods Ecol. Evol.* **3**, 217–223. (doi:10.1111/j.2041-210X.2011.00169.x)
53. Ackerly D. 2009 Colloquium papers: conservatism and diversification of plant functional traits: evolutionary rates versus phylogenetic signal. *Proc. Natl Acad. Sci.* **106**, 19 699–19 706. (doi:10.1073/pnas.0901635106)
54. Bapst DW. 2012 paleotree: an R package for paleontological and phylogenetic analyses of evolution. *Methods Ecol. Evol.* **3**, 803–807. (doi:10.1111/j.2041-210X.2012.00223.x)
55. Paradis E, Claude J, Strimmer K. 2004 APE: analyses of phylogenetics and evolution in R language. *Bioinformatics* **20**, 289–290. (doi:10.1093/bioinformatics/btg412)
56. Freckleton RP, Jetz W. 2009 Space versus phylogeny: disentangling phylogenetic and spatial signals in comparative data. *Proc. R. Soc. B* **276**, 21–30. (doi:10.1098/rspb.2008.0905)
57. Freckleton RP. 2002 On the misuse of residuals in ecology: regression of residuals vs. multiple regression. *J. Anim. Ecol.* **71**, 542–545. (doi:10.1046/j.1365-2656.2002.00618.x)
58. Orme CDL, Freckleton RP, Thomas GH, Petzoldt T. 2012 *The caper package—comparative analysis of phylogenetics and evolution in R*. See http://cran.r-project.org/web/packages/caper/index.html.
59. Ishii HS, Harder LD. 2012 Phenological associations of within- and among-plant variation in gender with floral morphology and integration in protandrous *Delphinium glaucum*. *J. Ecol.* **100**, 1029–1038. (doi:10.1111/j.1365-2745.2012.01976.x)
60. Conner JK, Sterling A. 1985 Testing hypotheses of functional relationships: a comparative survey of correlation patterns among floral traits in five insect-pollinated plants. *Am. J. Bot.* **82**, 1399–1406. (doi:10.2307/2445866)
61. Gómez-Robles A, Polly PD. 2012 Morphological integration in the hominin dentition: evolutionary, developmental, and functional factors. *Evolution* **66**, 1024–1043. (doi:10.1111/j.1558-5646.2011.01508.x)
62. Klingenberg CP, Duttke S, Whelan S, Kim M. 2012 Developmental plasticity, morphological variation and evolvability: a multilevel analysis of morphometric integration in the shape of compound leaves. *J. Evol. Biol.* **25**, 115–129. (doi:10.1111/j.1420-9101.2011.02410.x)
63. Klingernberg CP, Marugán-Lobón J. 2013 Evolutionary covariation in geometric morphometric data: analyzing integration, modularity, and allometry in a phylogenetic context. *Syst. Biol.* **62**, 591–610. (doi:10.1093/sysbio/syt025)
64. Gómez JM, Bosch J, Perfectti F, Fernandez JD, Abdelaziz M, Camacho JPM. 2008 Spatial variation in selection on corolla shape in a generalist plant is promoted by the preference patterns of its local pollinators. *Proc. R. Soc. B* **275**, 2241–2249. (doi:10.1098/rspb.2008.0512)
65. Thompson JN. 2009 Which ecologically important traits are most likely to evolve rapidly? *Oikos* **118**, 1281–1283. (doi:10.1111/j.1600-0706.2009.17835.x)
66. Davis CC. 2008 Floral evolution: dramatic size change was recent and rapid in the world's largest flowers. *Curr. Biol.* **18**, R1102–R1104. (doi:10.1016/j.cub.2008.10.011)
67. Revell LJ, Harmon LJ, Collar DC. 2008 Phylogenetic signal, evolutionary process, and rate. *Syst. Biol.* **57**, 591–601. (doi:10.1080/10635150802302427)

Gómez, JM *et al.* 2014. The role of pollinator diversity in the evolution of corolla-shape integration in a pollination-generalist plant clade. *Phil. Trans. R. Soc. B.* **369** doi: 10.1098/rstb.2013.0257

SUPPLEMENTARY MATERIAL

Table S1. Location and sample size of studied *Erysimum* species. Number of sample populations refers to the number of populations where flower visitor counts were made. Number of sampled individuals refers to the number of individual plants used for geometric morphometric analyses. *Erysimum* taxonomy follows Gonzalo-Nieto (1993), Heywood et al. (1964), Polatschek (1982), Giardina et al. (2007), Abdelaziz et al. (2011).

Species	Geographical distribution	Studied locality	Habitat	Number of sampled populations	Number of sampled individuals	Number sampled insects
E. baeticum baeticum (Heywood) Polatschek	Baetic Mountains (Spain)	Sierra Nevada (Almería, Spain)	Alpine	3	60	861
E. baeticum bastetanum Blanca & C. Morales	Baetic Mountains (Spain)	Sierra de Baza (Granada, Spain)	Mid-mountain	3	60	572
E. bicolor DC.	Macaronesia	Tenerife Island (Canary Islands, Spain)	Lowland	1	26	565
E. bonannianum C. Presl.	Sicily	Florenta (Sicily, Italy)	Mid-mountain	3	72	424
E. cazorlense (Heywood) Holub	Baetic Mountains (Spain)	Sierra de Segura (Jaén, Spain)	Mid-mountain	1	30	174
E. cheiranthoides L.	Western Europe	Waltersdorf (Brandeburg, Germany)	Lowland	1	30	241
E. cheiri (L.) Crantz	Europe	Oberstein (Renania, Germany)	Lowland	2	17	74
E. collisparsum Jord.	North-East Italy South France	Millesimo (Savona, Liguria, Italy)	Lowland	1	30	160
E. crassistylum C. Presl.	Central-East Mediterranean	Mt San Angelo (Puglia, Italy)	Lowland	2	63	100
E. crepidifolium Rchb.	Central Europe	Hollfeld (Bavaria, Germany)	Lowland	2	40	137
E. duriaei Boiss.	Cantabric Mountains (Spain)	Picos de Europa (Oviedo, Spain)	Alpine	2	30	165
E. etnense Jord.	Sicily	Mt Etna (Catania, Sicily, Italy)	Mid-mountain	2	60	516
E. fitzii Polatschek	Baetic Mountains (Spain)	Sierra de Pandera (Jaén, Spain)	Mid-mountain	2	60	272
E. gomezcampoi Polatschek	East Iberian Peninsula	Font Roja (Alicante, Spain)	Mid-mountain	2	60	382
E. gorbeanum Polatschek	North Iberian Peninsula	Sierra de la Demanda (Burgos, Spain)	Mid-mountain/Alpine	1	30	167
E. incanum Kunze	Southern Europe and North Africa	Baza (Granada, Spain)	Aridlands	2	60	
E. jugicola Jord.	Alps	Gran Paradiso National Park (Aosta, Italy)	Mid-mountain	1	30	209
E. lagascae Rivas Goday & Bellot	Iberian Central System	Gredos Mountains (Toledo, Spain)	Mid-mountain	2	60	324
E. linifolium (Pourr . ex Pers.) J. Gay	North-West Iberian Peninsula	Bierzo (Lugo, Spain)	Mid-mountain	2	27	
E. mediohispanicum Polatschek	Central-East Iberian Peninsula	Sierra Nevada (Granada, Spain)	Mid-mountain	2	60	1411
E. metlesicsii Polatschek	Sicily	Marianopolis (Sicily, Italy)	Lowland	1	30	99
E. merxmuelleri Polatschek	Iberian Central System	Gredos Mountains (Avila, Spain)	Mid-mountain	2	60	498
E. myriophyllum Lange	Baetic Mountains (Spain)	Sierra de Huétor (Granada, Spain)	Mid-mountain	2	62	816
E. nervosum Pomel	Atlas mountains	Ifrane (Meknès-Tafilalet , Morocco)	Alpine	2	60	632

E. nevadense Reut.	Baetic Mountains (Spain)	Sierra Nevada (Granada, Spain)	Alpine	2	60	1324
*E. geisleri** Polatschek	South-Western Alps and Prealps	Mt Ventoux (Provence, France)	Alpine	2	32	223
E. odoratum Ehrh.	North-Central Europe	Pottenstein (Bavaria, Germany)	Lowland	2	60	432
E. penyalarense (Pau) Polatschek	Iberian Central System	Guadarrama Mountains (Madrid, Spain)	Alpine	2	34	230
E. popovii Rothm.	Baetic Mountains (Spain)	Sierra de Cogollos (Granada, Spain)	Mid-mountain	2	65	484
E. pseudorhaeticum Polatschek	Central Italy	Collagna (Reggio-Emilia, Italy)	Mid-mountain	2	62	344
E. rhaeticum Kunze ex Willk.	Alps	Chiavenna (Sondrio, Lombardy, Italy)	Mid-mountain	2	60	273
E. riphaeanum Lorite et al.	Rif mountains (Morocco)	Talassemtane (Chefchaouen, Morocco)	Mid-mountain	2	60	288
E. rondae Polatschek	Baetic Mountains (Spain)	Grazalema (Cádiz, Spain)	Mid-mountain	1	59	259
E. ruscinonense Jord.	North-East Iberian Peninsula	Montseny (Barcelona, Spain)	Mid-mountain	2	60	578
E. scoparium Wettst.	Macaronesia	Tenerife (Canary Islands, Spain)	Alpine	2	30	205
E. semperflorens Wettst.	North Africa	Essaouira (Marrakech-Tensift-Al Haouz, Morocco)	Lowland	1	30	91
E. sepkiae Polatschek	Pyrenees	Pyreness (Huesca, Spain)	Alpine	1		
E. sylvestre Def.	Alps	Hohe Tauern (Sajahütte, Austria)	Alpine	1	58	
E. virgatum Roth	Western and Central Europe	Alps (Hautes-Alpes, France)	Mid-mountain	1		
E. wilczekianum Maire	Atlas Mountains	Ifrane (Meknès-Tafilalet, Morocco)	Alpine	2	60	212

* formerly *Erysimum ochroleucum*

Taxonomical references:

Abdelaziz, M., Lorite, J., Muñoz-Pajares, A. J., Herrador, M. B., Perfectti, F. & Gómez, J. M. 2011 Using complementary techniques to distinguish cryptic species: A new *Erysimum* (Brassicaceae) species from North Africa. *Am. J. Bot.* **98**, 1049–1060.

Giardina, G., Raimondo F. M., Spadaro V. 2007. A Catalogue of plants growing in Sicily. *Bocconea* **20**, 5-582.

Heywood, V. H., Valentine, D. H., Tutin, T. G. & Burges, N. A. 1964 *Flora Europaea*. Cambridge University Press.

Nieto Feliner, G. 1993. *Erysimum* in Castroviejo et al. (1993). Flora Iberica Vol. 4. CSIC.

Polatschek, A. 1982. *Erysimum*. Pp. 382-389 in: Pignatti, S., Flora d'Italia, 1. Bologna.

Polatschek, A. 2008. *Erysimum* (Brassicaceae). 15 neue Arten aus Europa, N-Afrika und Asien. *Ann. Naturhist. Mus. Wien* **109B**, 147-165.

Table S2. GenBank Accession numbers of DNA sequences (*ITS*, *ndhF*, *trnT-trnL* spacer) used to obtain the phylogenetic relationships between the studied species of *Erysimum*.

Species	***ITS sequences***	***ndhF sequences***	***trnT-trnL sequences***
E. baeticum baeticum	KF445238	KF445274	KF445310
E. baeticum bastetanum	KF445237	KF445273	KF445309
E. bicolor	KF445240	KF445276	KF445312
E. bonannianum	KF445241	KF445277	KF445313
E. cazorlense	KF445242	KF445278	KF445314
E. cheiranthoides	KF445243	KF445279	KF445315
E. collisparsum	KF445244	KF445280	KF445316
E. crassistylum	KF445246	KF445282	KF445318
E. crepidifolium	KF445245	KF445281	KF445317
E. duriaei	KF445247	KF445283	KF445319
E. etnense	KF445239	KF445275	KF445311
E. fitzii	KF445248	KF445284	KF445320
E. geisleri	KF445260	KF445296	KF445332
E. gomezcampoi	KF445249	KF445285	KF445321
E. gorbeanum	KF445250	KF445286	KF445322
E. incanum	HM235724/HM235736	HM235748	HM235760
E. jugicola	KF445251	KF445287	KF445323
E. lagascae	KF445253	KF445289	KF445325
E. linifolium	KF445252	KF445288	KF445324
E. mediohispanicum	KF445254	KF445290	KF445326
E. merxmuelleri	KF445256	KF445292	KF445328
E. metlesicsii	KF445255	KF445291	KF445327
E. myriophyllum	KF445257	KF445293	KF445329
E. nervosum	HM235726/HM235738	HM235750	HM235762
E. nevadense	KF445258	KF445294	KF445330
E. odoratum	KF445259	KF445295	KF445331
E. passgalense	KF445262	KF445298	KF445334
E. penyalarense	KF445263	KF445299	KF445335
E. popovii	KF445261	KF445297	KF445333
E. pseudorhaeticum	KF445264	KF445300	KF445336
E. rhaeticum	KF445266	KF445302	KF445338
E. riphaeanum	HM235728/HM235740	HM235752	HM235764
E. rondae	KF445265	KF445301	KF445337
E. ruscinonense	KF445267	KF445303	KF445339
E. scoparium	KF445269	KF445305	KF445341
E. seipkae	KF445268	KF445304	KF445340
E. semperflorens	KF445270	KF445306	KF445342
E. sylvestre	KF445271	KF445307	KF445343
E. virgatum	KF445272	KF445308	KF445344
E. wilczekianum	HM235734/HM235746	HM235758	HM235770

Table S3. Ancestral reconstruction of corolla shape integration using maximum likelihood approach. N= number of phylogenetic trees where the trait was reconstructed; Mean= mean trait value per node; SD= standard deviation of the trait value per node across the entire set of phylogenetic trees

Node	N	Mean	SD	Minimum	Maximum
38	6400	0.1431	0.0039	0.1299	0.1740
39	6400	0.1422	0.0048	0.1121	0.1730
40	6400	0.1479	0.0039	0.1136	0.1711
41	6400	0.1485	0.0102	0.1129	0.1991
42	6400	0.1497	0.0168	0.1121	0.2013
43	6400	0.1485	0.0171	0.1110	0.1936
44	6400	0.1512	0.0212	0.1151	0.1933
45	6400	0.1496	0.0170	0.1069	0.2313
46	6400	0.1467	0.0194	0.1034	0.2357
47	6400	0.1563	0.0119	0.1135	0.2373
48	6400	0.1601	0.0178	0.1115	0.2411
49	6400	0.1631	0.0184	0.1094	0.2521
50	6400	0.1696	0.0198	0.1008	0.2525
51	6400	0.1645	0.0203	0.1019	0.2479
52	6400	0.1609	0.0203	0.1012	0.2466
53	6400	0.1568	0.0214	0.1020	0.2396
54	6400	0.1567	0.0271	0.1021	0.2576
55	6400	0.1593	0.0297	0.1007	0.2530
56	6400	0.1616	0.0298	0.1020	0.2560
57	6400	0.1558	0.0295	0.1006	0.2570
58	6400	0.1490	0.0255	0.1003	0.2475
59	6400	0.1485	0.0276	0.0996	0.2409
60	6400	0.1519	0.0313	0.1003	0.2500
61	6400	0.1541	0.0317	0.1001	0.2580
62	6400	0.1535	0.0295	0.1006	0.2549
63	6400	0.1504	0.0277	0.1022	0.2512
64	6400	0.1483	0.0290	0.0981	0.2512
65	6400	0.1509	0.0342	0.1003	0.2544

66	6400	0.1536	0.0370	0.1002	0.2586
67	6400	0.1609	0.0350	0.1008	0.2588
68	6400	0.1471	0.0216	0.0984	0.2493
69	6400	0.1445	0.0216	0.0991	0.2400
70	6400	0.1464	0.0282	0.0998	0.2458
71	6400	0.1480	0.0315	0.1012	0.2519
72	6400	0.1482	0.0332	0.1033	0.2556
73	6400	0.1496	0.0343	0.1003	0.2545

Table S4. Ancestral reconstruction of corolla shape integration using Bayesian approach. N= number of phylogenetic trees where the trait was reconstructed; Mean= mean trait value per node; SD= standard deviation of the trait value per node across the entire set of phylogenetic trees

Node	N	Mean	Std Dev	Minimum	Maximum
38	6400	0.1433	0.0081	0.1080	0.1759
39	6400	0.1423	0.0081	0.1072	0.1752
40	6400	0.1480	0.0071	0.1098	0.1753
41	6400	0.1486	0.0114	0.1055	0.2011
42	6400	0.1499	0.0176	0.1093	0.2062
43	6400	0.1484	0.0175	0.1077	0.1961
44	6400	0.1510	0.0214	0.1097	0.2006
45	6400	0.1500	0.0175	0.1099	0.2221
46	6400	0.1472	0.0197	0.1104	0.2363
47	6400	0.1561	0.0129	0.1087	0.2380
48	6400	0.1597	0.0180	0.1095	0.2418
49	6400	0.1627	0.0188	0.1098	0.2530
50	6400	0.1692	0.0205	0.1006	0.2486
51	6400	0.1642	0.0207	0.1010	0.2479
52	6400	0.1604	0.0211	0.1010	0.2394
53	6400	0.1559	0.0220	0.1023	0.2385
54	6400	0.1557	0.0268	0.1023	0.2581
55	6400	0.1591	0.0296	0.1024	0.2531
56	6400	0.1609	0.0297	0.1020	0.2562
57	6400	0.1555	0.0294	0.1008	0.2569
58	6400	0.1487	0.0255	0.1003	0.2450
59	6400	0.1483	0.0280	0.0996	0.2408
60	6400	0.1520	0.0309	0.1007	0.2511
61	6400	0.1542	0.0316	0.1010	0.2581
62	6400	0.1534	0.0293	0.1006	0.2550
63	6400	0.1504	0.0275	0.1016	0.2453
64	6400	0.1485	0.0294	0.0973	0.2511
65	6400	0.1514	0.0343	0.1002	0.2546

Node	N	Mean	Std Dev	Minimum	Maximum
66	6400	0.1547	0.0373	0.0998	0.2566
67	6400	0.1611	0.0354	0.1009	0.2587
68	6400	0.1471	0.0215	0.0976	0.2408
69	6400	0.1447	0.0219	0.1028	0.2402
70	6400	0.1463	0.0278	0.1009	0.2470
71	6400	0.1487	0.0321	0.1021	0.2520
72	6400	0.1488	0.0336	0.1038	0.2553
73	6400	0.1493	0.0339	0.1029	0.2528

Figure S1. Phylogenetic relationships between the studied species of *Erysimum*. The strict consensus tree based on Bayesian inference. Bayesian support indices are shown above the branches.

Figure S2. Differences in the percentage of shape variance explained by each GPA principal component in four *Erysimum* species differing in corolla shape integration (*E. wilczekianum* corolla shape integration= 0.045, *E. myriophyllum* = 0.140, *E. pseudorhaeticum* = 0.079, E. *rhaeticum* = 0.167). Only the first 30 PCs are represented, because most of the remaining PCs explained 0% of the variance in shape. The among-individual dispersion of landmarks around the consensus is also shown.

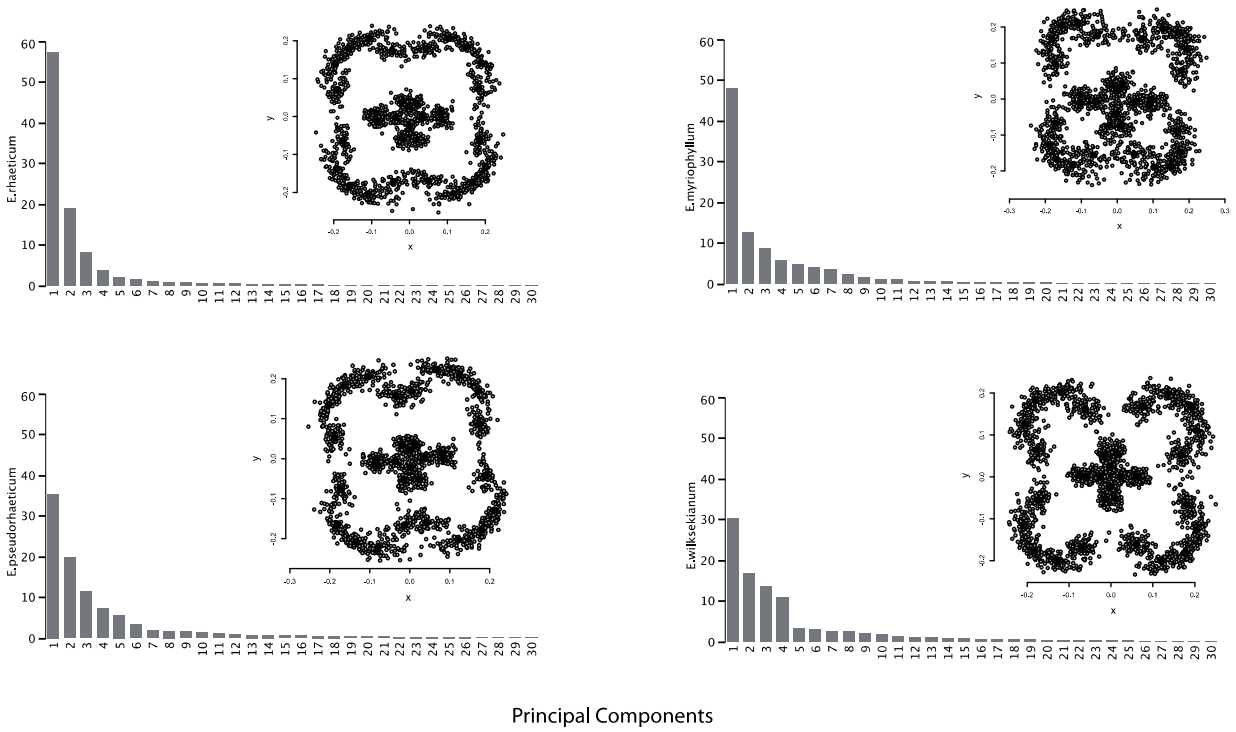

Figure S3. Traitgram showing the changes in the degree of pollination generalization, expressed as number of pollinator species per population across plant species, in relation with the phylogenetic relatedness of the *Erysimum* species.